HNPS Advances in Nuclear Physics

Vol 30 (2024)

HNPS2023

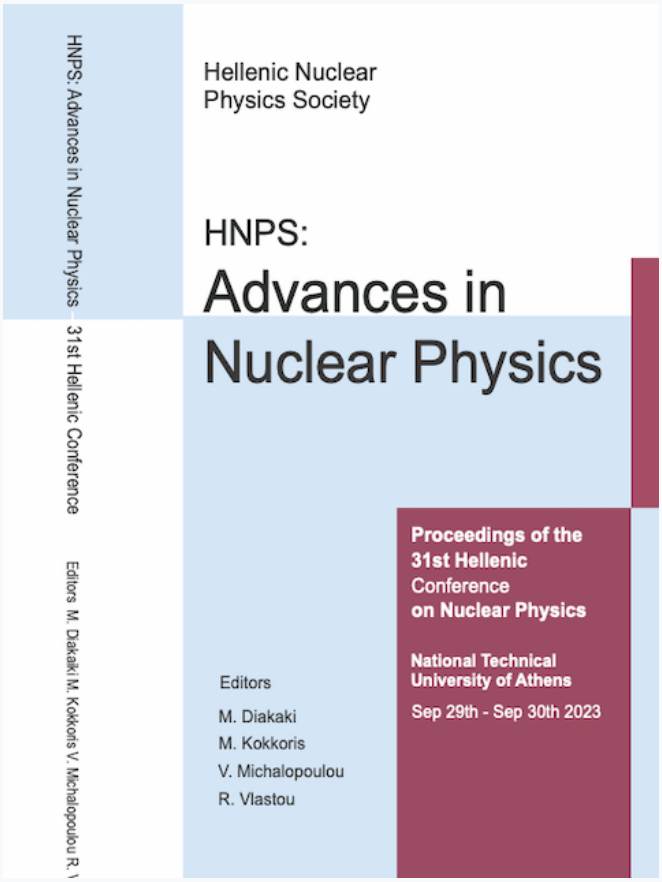

Neutron dosimetry at HK-1 beam line of LVR-15 reactor for biomedical sample irradiations

Antigoni Kalamara, Sofia Georgiou, Konstantinos L. Stefanopoulos, Ion E. Stamatelatos, John A. Kalef-Ezra, Miroslav Vinš, Vit Klupák, Michaela Rabochová, Jaroslav Šoltés, Theodossis Theodossiou

doi: 10.12681/hnpsanp.6285

To cite this article:

Kalamara, A., Georgiou, S., Stefanopoulos, K. L., Stamatelatos, I. E., Kalef-Ezra, J. A., Vinš, M., Klupák, V., Rabochová, M., Šoltés, J., & Theodossiou, T. (2024). Neutron dosimetry at HK-1 beam line of LVR-15 reactor for biomedical sample irradiations. *HNPS Advances in Nuclear Physics*, *30*, 207–210. https://doi.org/10.12681/hnpsanp.6285

Neutron dosimetry at HK-1 beam line of LVR-15 reactor for biomedical sample irradiations

A. Kalamara[1,2,*], S. Georgiou[1], K.L. Stefanopoulos[2], I.E. Stamatelatos[1], J.A. Kalef-Ezra[3], M. Vinš[4], V. Klupák[4], M. Rabochová[4], J. Šoltés[4], T. Theodossiou[5]

[1] *INRASTES, NCSR "Demokritos", 15310 Aghia Paraskevi, Greece*
[2] *INN, NCSR "Demokritos", 15310 Aghia Paraskevi, Greece*
[3] *Medical Physics Laboratory, School of Health Sciences, University of Ioannina, Ioannina, 45110, Greece*
[4] *Research Center Rez, Hlavní 130, 250 68, Husinec-Řež, Czech Republic*
[5] *Institute for Cancer Research, Oslo University Hospital, Oslo, Norway*

Abstract The HK-1 neutron beam line at the LVR-15 reactor in ÚJV Řež, Czech Republic, was used for *in vitro* cell studies carried out in the framework of the FRINGE project, aiming on the development of a novel neutron capture therapy technique using Gd containing compounds. The neutron fluence rate close the HK-1 beam exit was experimentally assessed. Neutron fluence rate data were combined with Monte Carlo simulations performed using the MCNP 6.1 code, to model a well-type vial containing a thin layer of cells, with and without Gd, as well as the supporting media. Aim of the study was to evaluate the energy deposited by the neutrons in the cell monolayers and delineate the contribution of the various dose components in an attempt to interpretate the findings of the *in vitro* studies.

Keywords cancer therapy, neutron, Monte Carlo simulations, dosimetry

INTRODUCTION

In the framework of the HORIZON 2020 FET-OPEN research project entitled “Fluoresence and Reactive oxygen Intermediates by Neutron Generated electronic Excitation as a foundation for radically new cancer therapies (FRINGE)” [1], the HK-1 neutron beam line at the LVR-15 reactor in ÚJV Řež, Czech Republic was used for *in vitro* irradiation studies [2]. Specifically, photosensitive Gd-containing compounds were incubated with different cancer cell types and irradiated.

Scope of the present work was to evaluate the energy imparted to the cells and delinate the dose contribution of protons, heavy charged particles and electrons, for interpreting the findings of the radiobiological experiments. The neutron fluence rate at the HK-1 neutron beam line was measured using activation foils. In addition, a model approximating the FRINGE *in vitro* irradiations was developed using the MCNP 6.1 code [3] to predict the energy deposition.

EXPERIMENT

Au, Zn and Cu foils were irradiated for 4 h and 16 min and their induced activities were measured by means of a 25% relative efficiency calibrated HPGe detector. The mean thermal neutron fluence rate obtained by using several reactions was found to be $(5.5 \pm 0.1)\times10^{7}$ cm^{-2} s^{-1} at 10 MW$_{th}$ reactor power (Table 1).

Table 1. *Reactions and experimental neutron flux values obtained by activation foils*

Reaction	Φ (n/cm^2 s)	δΦ (n/cm^2 s)
^{197}Au(n,γ)^{198}Au	5.10E+07	1.42E+05
^{64}Zn(n,γ)^{65}Zn	5.64E+07	2.18E+06
^{68}Zn(n,γ)^{69m}Zn	5.61E+07	3.63E+05
^{63}Cu(n,γ)^{64}Cu	5.50E+07	7.63E+05

* Corresponding author: *a.kalamara@ipta.demokritos.gr*

SIMULATIONS

Monte Carlo simulations were performed by means of the MCNP 6.1 code to evaluate the energy deposited in the cell monolayer by using the scoring tallies (+f6, *f8 and f4). Each cell holder (Fig. 1) allows for the simultaneous irradiation of cells present in a 6×3 well-plate array, with well dimensions 5.7 mm × 6.1 mm × 6.8 mm. Neutrons pass only through a polyethylene window of 180 μm thickness before reaching the cells, which were described as a 20 μm–thick monolayer of ICRU soft-tissue composition [4]. The medium layer, shown in Fig. 2(b), was described as H_2O, since preliminary simulations using H_2O and soft tissue in the medium volume resulted in differences of less than 5% in the calculated dose at the cell layer.

The HK-1 neutron spectrum divided in four energy regions and the modeled geometry are shown in Figs. 2(a) and 2(b), respectively. It is noted that the neutron spectrum in Fig. 2(a) includes interactions with the neutron beam line materials, such as beam modifiers, shielding and collimator. However, gamma rays originating either directly from the reactor core or neutron interactions with the in pile collimator and shielding materials were not taken into account in the present study.

Figure 1. *Holder used for the cells irradiations (6x3 well-plate array) [5]*

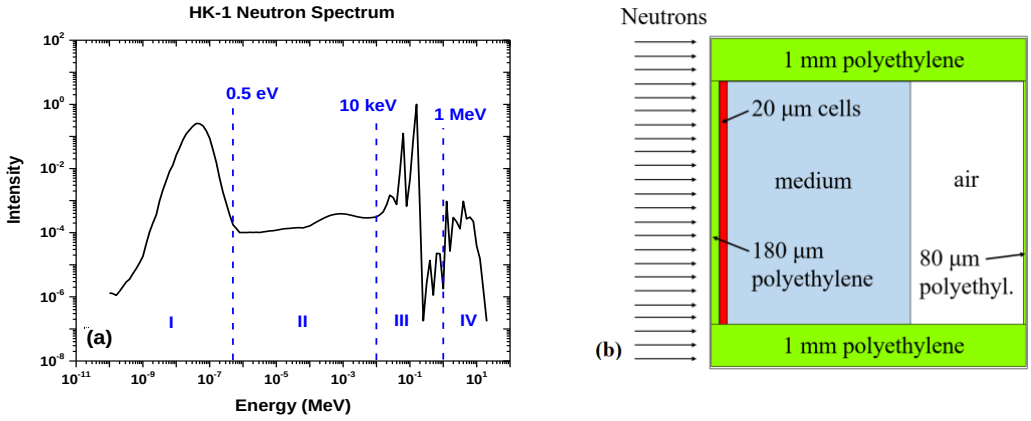

Figure 2. (a) *HK-1 beam line neutron spectrum used in the MCNP simulations. (b) Geometry described in the MCNP for the single well simulation (not in scale).*

The energy deposition in the cell monolayer by the various high LET particles (secondary protons and other heavy charged particles, +f6 tally) in the cell monolayer, as well as the deposition by the secondary photons and electrons only (*f8 tally), were inserted to Eqs. (1) and (2), respectively, along with the total incoming neutron fluence (Σf4) for the calculation of the corresponding dose rates in Gy/h.

$$\text{High LET} \rightarrow \text{Dose Rate}\left(\frac{\text{Gy}}{\text{h}}\right) = \frac{+\text{f6}\left(\frac{\text{MeV}}{\text{g n}}\right)\cdot\left(\frac{1.6\cdot10^{-13}\ J/MeV}{0.001\ kg/g}\right)}{\Sigma_{total}\,\text{f4}\left(\frac{1}{\text{cm}^2\,\text{n}}\right)} \cdot \Phi_{exper.}\left(\frac{\text{n}}{\text{cm}^2\,\text{s}}\right) \cdot 3600\ \text{s} \qquad (1)$$

$$\text{Low LET} \rightarrow \text{Dose Rate}\left(\frac{\text{Gy}}{\text{h}}\right) = \frac{{}^{*}\text{f8}\left(\frac{\text{MeV}}{\text{n}}\right)}{cell\ layer\ mass\ (g)} \cdot \frac{\left(\frac{1.6\cdot10^{-13}\ J/MeV}{0.001\ kg/g}\right)}{\sum_{total}\text{f4}\left(\frac{1}{\text{cm}^2\ \text{n}}\right)} \cdot \Phi_{exper.}\left(\frac{\text{n}}{\text{cm}^2\ \text{s}}\right) \cdot 3600\ \text{s} \qquad (2)$$

The dose rates due to high and low LET radiations divided in the four energy groups are shown in Tables 2 and 3, respectively. The results for secondary photons and electrons are associated with larger uncertainties, since they deposit most of their energy outside the target cell monolayer.

Table 2. *Dose rates calculated with Eq. (1) for neutrons* and *secondary protons* and *heavy ions (+f6 tally) at the HK-1 beam line of the LVR-15 reactor at ÚJV Řež*

Energy Region		Without Gd		With Gd		Ratio of Dose Rates
		Dose Rate (Gy/h)	Relative Error	Dose Rate (Gy/h)	Relative Error	$\frac{With\ Gd}{Without\ Gd}$
I	E < 0.5 eV	7.6E-10	1.69 %	9.3E-10	1.93 %	1.22 ± 0.03
II	0.5 eV < E < 10 keV	0.101	0.53 %	0.110	0.47 %	1.09 ± 0.01
III	10 keV < E < 1 MeV	0.490	0.38 %	0.463	0.38 %	0.94 ± 0.01
IV	E > 1 MeV	0.003	1.56 %	0.007	0.99 %	2.60 ± 0.05

Table 3. *Dose rates calculated with Eq. (2) for secondary photons and electrons (*f8 tally - divided by the mass of the scoring volume) at the HK-1 beam line of the LVR-15 reactor at ÚJV Řež*

Energy Region		Without Gd		With Gd		Ratio of Dose Rates
		Dose Rate (Gy/h)	Relative Error	Dose Rate (Gy/h)	Relative Error	$\frac{With\ Gd}{Without\ Gd}$
I	E < 0.5 eV	3.4E-11	2.26 %	2.4E-09	1.67 %	69.3 ± 2.0
II	0.5 eV < E < 10 keV	0.0006	26.92 %	0.0051	27.6 %	8.00 ± 3.08
III	10 keV < E < 1 MeV	0.0020	15.59 %	0.0265	14.7 %	13.5 ± 2.9
IV	E > 1 MeV	0.0000	-	0.0002	35.3 %	-

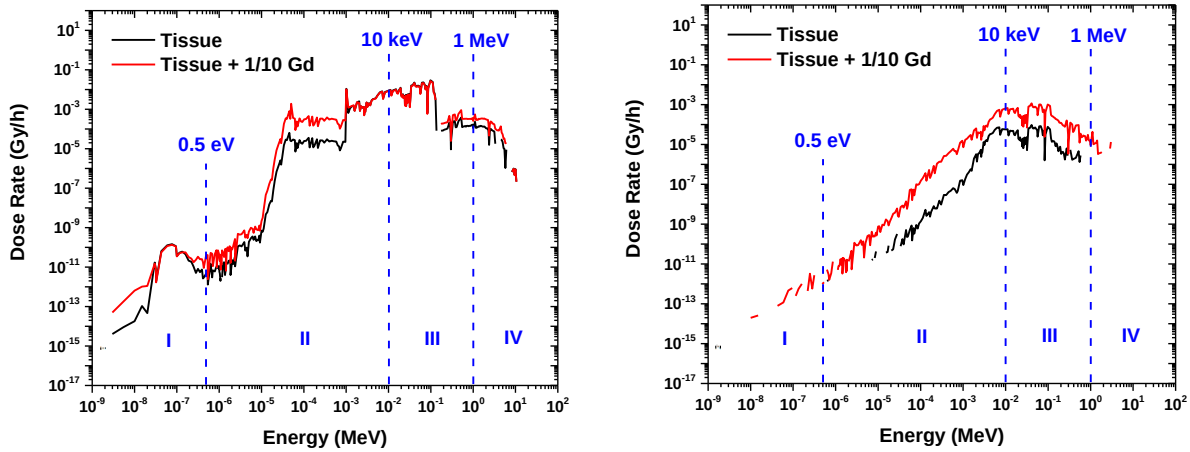

Figure 3. *(a) Dose rate calculated by Eq. (1), for +f6 tally, for all heavy charged particles. (b) Dose rate calculated by Eq. (2), for *f8 tally, for photons and electrons (due to the fact that the *f8 is given by MCNP in MeV/n, it is also divided with the mass of the scoring volume).*

Fig. 3 shows the dose rate in the cell layer due to the dose components per neutron energy bin. More specifically, Fig. 3(a) refers to the energy dissipated by the secondary protons and other charged particles (high LET dose component) and Fig. 3(b) due to the secondary photons and electrons (low LET component). In addition, black and red lines correspond to cells with 0% and 10% ^{nat}Gd mass concentration, respectively.

DISCUSSION AND CONCLUSIONS

The potential use of gadolinium agents in neutron capture therapy, mainly due to the high ^{155}Gd and ^{157}Gd thermal neuton capture cross sections (61 and 254 kb), was discussed in detail by Deagostino et al. [6]. In particular, the emitted Auger electrons (mainly of energy less than 25 keV) following a capture reaction may enhance the energy imparted at regions close to the capture site due to their short ranges in tissue [7-9]. However, the energy deposition at microscopic level [10] modifies biological response, an effect often quantified by the quantity relative biological efficacy, RBE. In case of capture reactions in gadolinium nuclei, most of the secondary radiations are of low LET.

In the present study it was found that the imparted energy was marginally modified by the gadolinium presence in the cell monolayer. Most of the dose absorbed due to irradiations to the HK-1 port is due to the impinging neutrons of energy 1 keV to 150 keV, a region of enhanced biological efficacy [11], and not due to thermal neutron capture reaction products. The gadolinium presence increased the contribution of the low LET dose component to the total dose just from 0.4% to 5.2%, despite the large capture propability. This finding is attributed to the fact that most of the released energy by the capture reactions produces photons and high energy electrons that deposit most of their energy outside the cell monolayer, of just ~0.8 mg in mass. It should be noted that in the present work a high Gd concentration was assumed in the simulation (10% ^{nat}Gd mass ratio), in order to amplify the Gd effect, if any, and to improve the calculation statistics.

Acknowledgments

This work was done in the framework of the FRINGE project (https://www.fringe-fetopen.eu/), which has received funding from the European Union's Horizon 2020 research and innovation programme under grant agreement No 828922. The presented results were obtained using the CICRR infrastructure, which is financially supported by the Ministry of Education, Youth and Sports - project LM2023041.

References

[1] FRINGE Project Website: https://www.fringe-fetopen.eu/
[2] M. Marek et al., App. Rad. Isot. 88, 157 (2014); doi: 10.1016/j.apradiso.2013.11.040
[3] Initial MCNP6 Release Overview MCNP6 Version 1.0, Los Alamos National Laboratory report LA-UR-13-22934 (2013)
[4] Composition of soft tissue (ICRP): https://physics.nist.gov/cgi-bin/Star/cmpos.pl?matno=261
[5] 6x3 well-plate: https://ibidi.com/chambered-coverslips/236--slide-18-well.html
[6] A. Deagostino et al., Future Med. Chem. 8, 899 (2016); doi: 10.4155/fmc-2016-0022
[7] G.A. Miller et al., Nucl. Tech. 103, 320 (1993); doi: 10.13182/NT93-A34855
[8] Z.B. Alfassi et al., J. Radioanal. Nucl. Chem. 240, 687 (1999), doi: 10.1007/bf02349436
[9] A. Ku et al, EJNMMI Radiopharmacy and Chemistry 4, 27 (2019), doi: 10.1186/s41181-019-0075-2
[10] S. Georgiou et al., HNPS Adv. Nucl. Phys. 30, 189 (2024), doi: 10.12681/hnpsanp.6282
[11] Hall et al., Rad. Res. 64, 245 (1975), doi: 10.2307/3574262